Bulgarian Chemical Communications, Volume 50, Special Issue J (pp. 114–122) 2018

Structural peculiarities of natural chabazite modified by $ZnCl_2$ and $NiCl_2$

L. T. Dimowa[1], I. Piroeva[2], S. Atanasova-Vladimirova[2], R. Rusew[1], B. L. Shivachev[1]*

[1] *Institute of Mineralogy and Crystallography, Bulgarian Academy of Sciences, "Acad. Georgi Bonchev" str., building 107, 1113 Sofia, Bulgaria*
[2] *Academician Rostislav Kaishev Institute of Physical Chemistry, "Acad. Georgi Bonchev" str., building 11, 1113 Sofia, Bulgaria*

Received March, 2018; Revised April, 2018

Chabazite single crystals were modified to NH_4^+, Zn^{2+} and Ni^{2+} chabazite forms and characterized by EDS/SEM, DTA/TG, FTIR and single crystal X-ray diffraction. The modification procedure includes successive conversion of the starting natural chabazite ($Na_{0.37}Ca_{1.56}$)$Al_{3.63}Si_{8.36}O_{24}.xH_2O$) into its ammonium form (NH4-CHA) where after the NH4-CHA form is converted to either zinc or nickel forms by ion-exchange with 1M $ZnCl_2$ and $NiCl_2$ water solutions at 100 °C. The EDS, FTIR and structural studies revealed remains of ammonium cations in Zn and Ni exchanged forms. The structural analyses disclosed that the water molecules present within the CHA framework tend to occupy sites that are usually related with nearby cation(s) sites. As the cation amounts required for the framework charge compensation is limited the water molecules amounts are also adjusting to this detail. The distribution of the water molecules in the 8-membered ring is of radial type.

Keywords: chabazite, microporous, single crystal, ion exchange.

INTRODUCTION

Crystalline open-framework materials such as aluminosilicate zeolites belong to a family of microporous materials that are attractive due to their rich structural chemistry and their various usage: as catalysts, in gas separation, ion exchange, low-*k* dielectric (thin film) materials, for H_2 and CO_2 gas storage [1–9]. Nowadays, in order to accommodate the industrial demand and increased technological requirements, the performed investigations target to improve the properties of existing crystalline open-framework materials and to discover new ones exhibiting better structure-property characteristics. This is achieved through modifications of currently available microporous materials and by the targeted design and synthesis of new ones [10–13]. The properties of "porous" materials are usually associated with their pore size, channel systems, thermal, mechanical and chemical stability. In the case of alumo-, titano-, zircono- and "other-" silicate zeolites used as catalysts, their catalytic activity is also related to the number and type of acid centers present in the structure [8, 14–16]. The efficiency of zeolites in catalytic reactions, gas separation, sorption, etc. applications can be better understood if in-depth knowledge of the structural features of existing materials is available. Therefore the investigations mainly target the pore size dimensions, the channel shape and size, the connectivity of the building blocks and the modification of the framework chemical composition [17, 18]. The detailed knowledge of structural features of existing materials is also critical for the design and synthesis of new ones. [19, 20]. However, in-depth structural characterization is a challenging task, because sufficiently bigger single crystals are difficult to grow. The synthesis of microporous materials usually produces microcrystalline powders, the characterization techniques are limited to powder diffraction, chemical analyses and spectroscopic methods. Moreover, typical optimization for industrial applications includes the maximization of the specific surface and/or volume of the samples through lowering the crystallite size e.g. going in the "nano" scale [13, 21, 22]. Thus most single crystal studies are performed on naturally grown samples. Chabazite is a natural microporous aluminosilicate with common formula $(M^{(I),(II)})_2Al_4Si_8O_{24}.nH_2O$ [23] where M = Na, K, Ag, Cs, Ca, Sr, Ba, Cd, Mn, Co, and Cu are the

* To whom all correspondence should be sent:
blshivachev@gmail.com

framework charge compensating cations. Natural chabazite(s) shows considerable variation in Si/Al ratio [24, 25]. Based on the dominant non-framework cation (natural) chabazite is usually referred as Ca-CHA, K-CHA, Na-CHA, Sr-CHA. The CHA structure consists of six-membered double rings (D6R) which are connected with tilted four-membered rings (4MR). As a result 8-membered twisted rings (8MR) with diameters of ~3.9 Å can be detected. The three-dimensional arrangement of the D6R (e.g. hexagonal prisms), 4MR and 8MR produces a $[4^{12}6^8 8^6]$ cavity 11.0 x 6.6 x 6.6 $Å^3$ in size, opened in all directions through the 8MR. Thus a three-dimensional system of channels is observed Fig. 1.

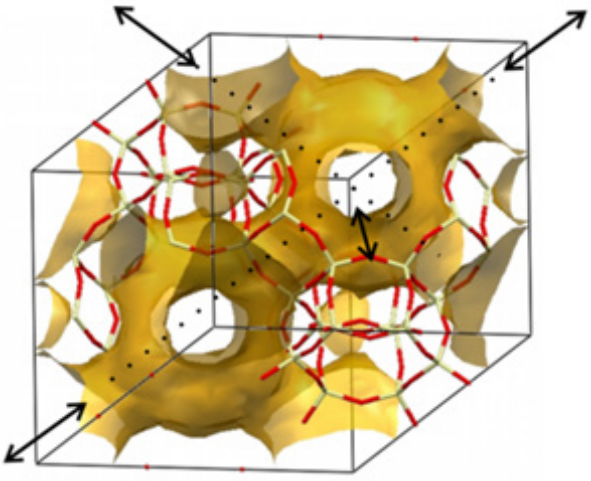

Fig. 1. Observation of the CHA framework surface (contoured with probe diameter of 2.4 Å) leading to the appearance of 3D channel system.

The large size of the CHA $[4^{12}6^8 8^6]$ cavity promotes the high sorption specificity for large cations such as alkali and alkaline Cs^+, K^+, Sr^{2+} [26]. CHA specific chemical and structural features (high specific surface and volume, thermal stability above 450 °C, simultaneous existence of small and large pores, voids and cavities, presence of acidic centers) makes it a material with likely application for bulk gas adsorption, gas separation, heavy oil cracking etc. Unfortunately, industrial scale deposits of chabazite are relatively rare and mostly unexploited (e.g. Bowie, Arizona, US; Gads Hill, Tasmania, AU). The natural chabazite deposits feature impurities e.g. parasite crystal phases, amorphous content etc. On the other hand, CHA with industrial quality (higher than 90%) can be easily produced from chabazite ore by combining gravity concentration, magnetic separation, semi-synthetic caustic digestion [27] or alternatively from commercial HY or K/NaY by "zeolite to zeolite conversion" [16, 20, 28] e.g. adjusting the Si/Al ratio using highly basic solutions (1–3M KOH) and additional amounts of SiO_2. The synthesis of CHA usually yields micro size crystals and thus hampers the detailed structural investigations. In this work we present structural studies of natural chabazite single crystals exchanged with ammonium, zinc and nickel cations.

EXPERIMENTAL

Materials

The starting material is a natural light gray chabazite (CHA) consisting of tightly packed single crystals with indeterminate habitus. The ion exchange was conducted in Teflon autoclaves using double distilled water (ddH_2O). For the preparation of exchange solutions the following Sigma-Aldrich reagents were used: NH_4Cl (A9434), $ZnCl_2$ (208086) and $NiCl_2$ x H_2O (364304).

Cation exchange

Initially natural chabazite was converted into ammonium form (NH4-CHA) by ion exchange with 1M NH_4Cl solution. Typically ~15 mg of CHA single crystals were added to 5 ml of 1M NH_4Cl and the mixture was heated to 90 °C with orbital shaking (40 rpm). After 40 hours the NH_4Cl solution was removed and replaced with fresh 1M NH_4Cl. This procedure (supplying fresh 1M NH_4Cl) was performed two times producing a total exchange time of 120 h (5 days). Finally, the NH_4Cl solution was discarded and the NH4-CHA was washed several times with ddH_2O. The resulting NH4-CHA was allowed to dry at room temperature for at least 24 hours. The zinc and nickel forms of chabazite were prepared starting from NH4-CHA by ion exchange with 1M $ZnCl_2$ and 1M $NiCl_2$ solutions at 100 °C for a total exchange time of 168 hours and using a similar procedure as for NH4-CHA (every 56 hours the 1M $ZnCl_2$ or 1M $NiCl_2$ solution were substituted with fresh ones).

Scanning electron microscopy

Scanning electron microscopy (SEM) microanalyses of the samples were performed on a JEOL JSM 6390 electron microscope (Japan) in conjunction with energy dispersive X-ray spectroscopy (EDS) Oxford INCA Energy 350, equipped with ultrahigh resolution scanning system (ASID-3D) in regimes of secondary electron image (SEI). The accelerating voltage was 15 kV, I ~65 nA, the pressure was of the order of 10^{-4} Pa. The single crys-

tals were directly placed on an adhesive carbon tape (Agarscientific) and coated with Au for 30 sec.

Differential thermal analysis (DTA) and thermo gravimetric (TG) losses

The DTA/TG data were obtained on a Setaram Setsys equipment. The experiment was carried out by placing approximately 2–3 mg of the CHA samples into a corundum crucible with heating of 10 °C min^{-1} from ambient temperature to 800 °C and under flowing argon gas (20 ml min^{-1}). Baseline curves, measured under the same experimental conditions were acquired to account for buoyancy effects. The peak fitting of the DTA data was performed with a Gaussian type of function using Fityk [29].

Fourier transform infrared spectroscopy (FTIR)

The FTIR spectra of the chabazite samples (KBr pellets) were recorded in the transmission mode at room temperature using a TENSOR 37 Bruker spectrometer in the 400–4000 cm^{-1} range. Before spectra collection the CHA samples were dried and crushed (grounded). The pellets were prepared using 50 mg KBr and 0.5 to 1 mg of (NH4, Zn, Ni)-CHA.

Single Crystal X-ray

Crystals of ammonium, zinc and nickel exchanged chabazite suitable for X-ray analyses were mounted on a glass capillary and all diffraction data were recorded from those crystals. Diffraction data were collected at room temperature by ω-scan technique, on an Agilent Diffraction SuperNovaDual four-circle diffractometer equipped with Atlas CCD detector using mirror-monochromatized Mo$K\alpha$ (λ = 0.7107 Å) radiation from micro-focus source. The determination of cell parameters, data integration scaling and absorption correction were carried out using the CrysAlisPro program package [30]. The structures were solved by direct methods [31] and refined by full-matrix least-square procedures on F^2 [31]. The natural and exchanged chabazite crystals were isotypical, space group R$\bar{3}m$ (No 166) with one molecule per asymmetric unit. A summary of the main fundamental crystal and refinement data is provided in Table 1.

Table 1. Important crystallographic and refinement details for ammonium, zinc and nickel exchanged chabazite

	NH4-CHA	Ni-CHA	Zn-CHA
Molecular weight	2784.84	2743.21	3056.50
Crystal system	Trigonal	Trigonal	Trigonal
Space group	R$\bar{3}$m	R$\bar{3}$m	R$\bar{3}$m
T(K)	290	290	290
Radiation, wavelength (Å)	Mo Kα, 0.71073	Mo Kα, 0.71073	Mo Kα, 0.71073
a (Å)	13.8520(3)	13.7972(5)	13.8485(7)
b (Å)	13.8520(3)	13.7972(5)	13.8485(7)
c (Å)	14.9061(3)	14.8847(7)	14.8504(8)
V(Å^3)	2476.96(9)	2453.88(17)	2466.5(2)
α (°)	90	90	90
β (°)	90	90	90
γ (°)	120	120	120
Z	1	1	1
F_{000}	1409.4	1498	1510
d (mg. m^{-3})	1.867	1.856	2.058
μ (mm^{-1})	0.554	1.340	1.590
Cell parameters	from 4113 reflections	from 4030 reflections	from 2508 reflections
Crystal habit, color	prism, colorless	prism, colorless	prism, colorless
Crystal size (mm^3)	0.30×0.28×0.27	0.30×0.28×0.27	0.29×0.26×0.23
Radiation source	SuperNova (Mo) X-ray	SuperNova (Mo) X-ray	SuperNova (Mo) X-ray
Monochromator	mirror	mirror	mirror
Data collection	ω scans	ω scans	ω scans
Reflections collected/I>2σ (I)	7385/1373	8111/1300	5710/1217
Parameters	55	61	68
R1 ($F^2 > 2\sigma(F^2)$)	0.037	0.052	0.049
wR2 (all data)	0.110	0.172	0.150
Extinction correction	none	none	none
$\Delta\rho_{max}$/ $\Delta\rho_{min}$ (e Å^{-3})	0.71/–0.70	1.38/–0.82	0.79/–0.61

DISCUSSION

The most employed and important technique used to modify zeolites is ion exchange. Ion-exchange properties of natural chabazite(s) have been well studied [9, 32, 33]. Normally the ion exchange process is not as lengthy but the use of single crystals, with limited exchange surface and almost certainly having crystal defects, hampering the ion exchange, implies longer exchange times and higher cation concentrations. As the 1M $ZnCl_2$ and $NiCl_2$ solutions have acidic character (pH around 4.7 at room temperature) the extension of the ion exchange period cannot be prolonged indeterminably due to the expected structural damage and eventual destruction of the CHA framework. The SEM images of the samples (Fig. 2) do not show noticeable degradation on the surface. This observation is further supported by conducted standardless EDS chemical composition analyses showing a persistent Si/Al molar ratio on a randomly nominated points on the surface of the samples (Table 2). This result is important from practical point of view, because it shows that no significant variation of the chabazite Si/Al framework is produced during the 7 days modification with acidic solutions of $ZnCl_2$ and $NiCl_2$. The positive/negative charge balance ($M^{+/2+}/Al^{-}$) is also very well-adjusted in natural, Zn- and Ni-CHA, being very close to the theoretical estimation. In the case of NH4-CHA the charge-balance should take into account that the exchange procedure may introduce both NH_4^+ and NH_3 species, indiscernible by EDS and most chemical analyses [14]. As SEM observation are carried out in vacuum (10^{-4} torr) the water molecules tend to leave the porous structure of chabazite and thus their content cannot be accurately deduced using standard EDS analyses (although the Oxford INCA Energy 350 detector outputs the oxygen amounts). For that reason TG analyses were preferred for the estimation of water content in zeolites. The DTA/TG results for the four samples, CHA, NH4-CHA, Zn-CHA and Ni-CHA are shown on Fig. 3. The TG curves of CHA and Ni-CHA show one stage weight losses while the NH4-CHA and Zn-CHA weight losses occur clearly in two stages. The principal weight losses

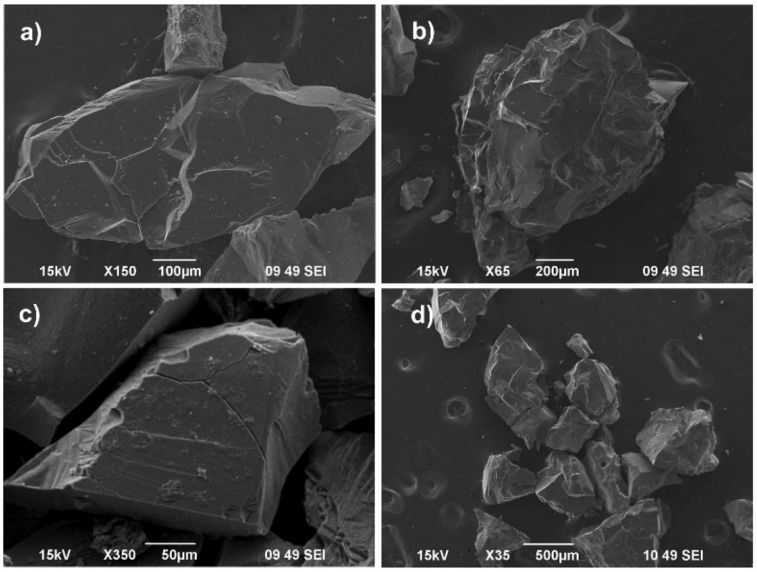

Fig. 2. SEM morphology of *a*) natural CHA, *b*) NH4-CHA, *c*) Zn-CHA, and *d*) Ni-CHA.

Table 2. Chemical compositions of natural and ammonium, zinc and nickel exchanged chabazite

Chabazite form	Extra-framework cations	Framework and waters	Si/Al ratio	Charge compensation
CHA natural	$(Ca_{1.59}Na_{0.37})$	$Al_{3.63}Si_{8.37}O_{24}$ nH_2O	2.30	$M^{+/2+}/Al^{-}$ = 3.48/3.63
NH4-CHA	$(N_{5.58})$	$Al_{3.52}Si_{8.48}O_{24}$ x nH_2O	2.41	NH_4^+/Al^{-} = 5.58/3.52
Ni-CHA	$(Ni_{1.43}\ N_{1.18})$	$Al_{3.96}Si_{7.82}O_{24}$ x nH_2O	1.87	$M^{+/2+}/Al^{-}$ = 4.04/3.96
Zn-CHA	$(Zn_{1.44}N_{0.96})$	$Al_{3.67}Si_{8.33}O_{24}$ x nH_2O	2.26	$M^{+/2+}/Al^{-}$ = 3.84/3.67

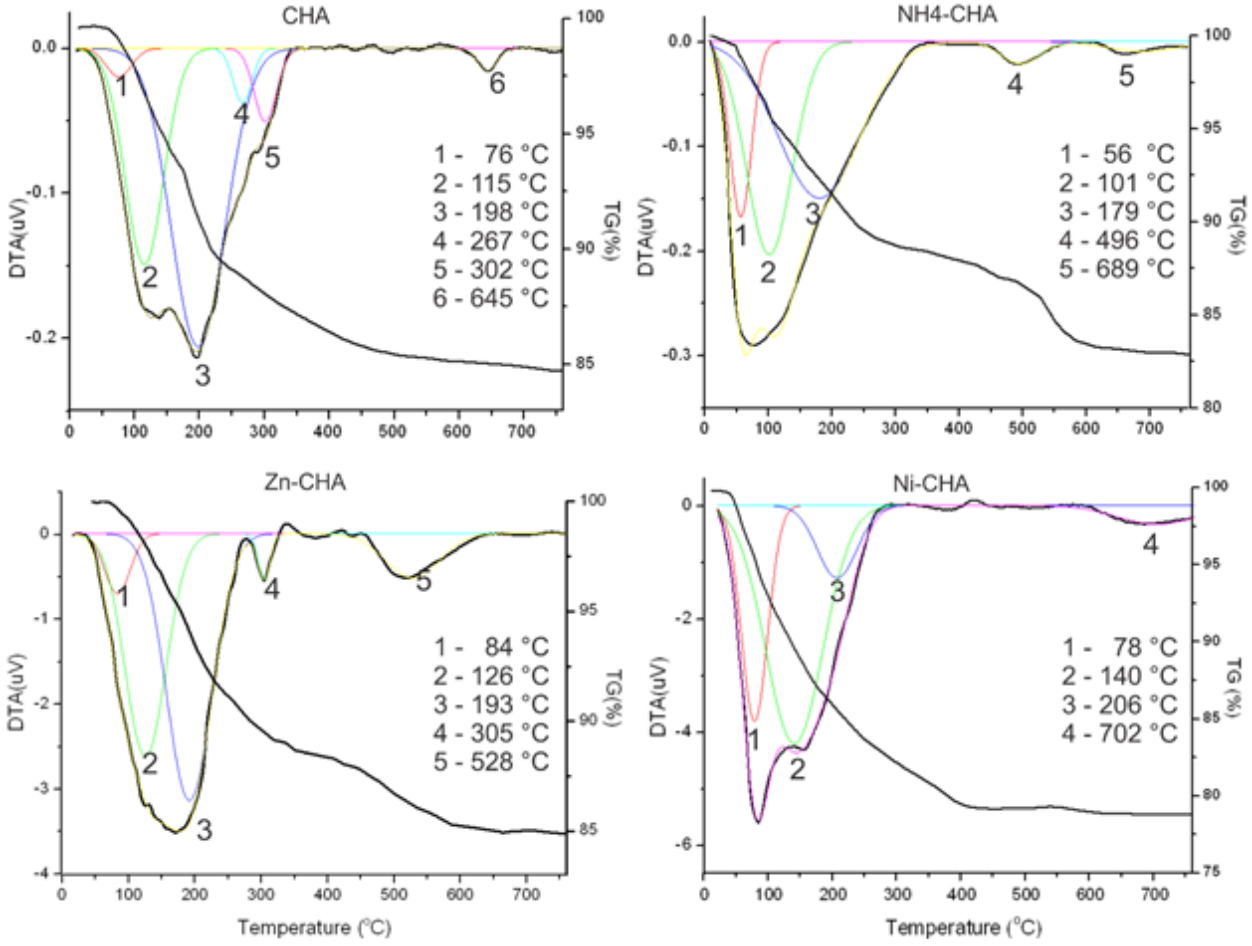

Fig. 3. DTA/TG data for a) natural CHA b) NH4-CHA c) Zn-CHA and d) Ni-CHA.

occur during the first stage (up to ~340 °C) and are mainly related to the release of water molecules and ammonium, in the case of NH4-CHA.

The tentative "peak fitting" of the DTA curves showed that the broad region (20 to ~340 °C) can be further subdivided (Fig. 3). In all four samples the fitting shows a peak in the 60–85 °C region that can be explained by "low temperature" desorption (release) of physisorbed water. The next two peaks (90–220 °C) are also common for the four CHA samples. The first one (~90 to 150 °C) can be explained by the breakup and release of hydrogen bonded water molecules, present in the channels. The second one (~150 to 220 °C) can be attributed to the more strongly coordinated H_2O molecules e.g. those that complement the cation coordination. Interestingly, in the cases of natural CHA and Zn-CHA the DTA data discloses *endothermic* effects in the region around 300 °C. As such effects are not present in the NH4- and Ni-CHA (Fig. 4) their assignment is a little bit delicate. An assumption is that due to the release of part of the H_2O molecules complementing the cation coordination sphere, the cations start to migrate and occupy positions closer to the negatively charged CHA framework sites (compensating their positive/negative charge). Thus the cations would "attract" even more strongly the remaining H_2O molecules and the release will occur even "slowly" and at higher temperatures. The process is beneficial for both the framework and the cations. Such explanation is also in agreement with TG data, showing a change of TG slope and thus the speed of weight losses. In the case of NH4-CHA the peak at ~490 °C is associated with the release of the ammonium (such effect is not observed in the other three samples). At higher temperatures (above 560 °C) the completion of the dehydration process and the release of remaining NH_4^+ are finalized.

The four FTIR spectra (natural, NH_4^+, Zn and Ni chabazite, Fig. 5) show analogous spectral bands related to the chabazite framework, NH_4^+, OH and H_2O molecules. The main feature is the presence of the bands associated with NH_4^+ vibration (~1420 cm^{-1} and a shoulder around 2800 cm^{-1})

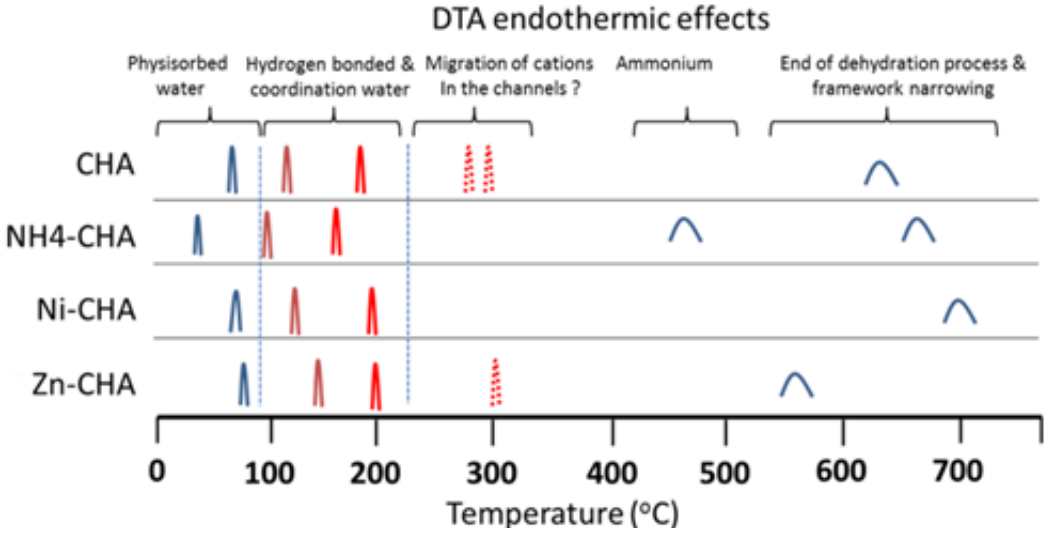

Fig. 4. DTA *endo* effects and associates processes in natural chabazite and exchanged NH4-CHA, Zn-CHA and Ni-CHA.

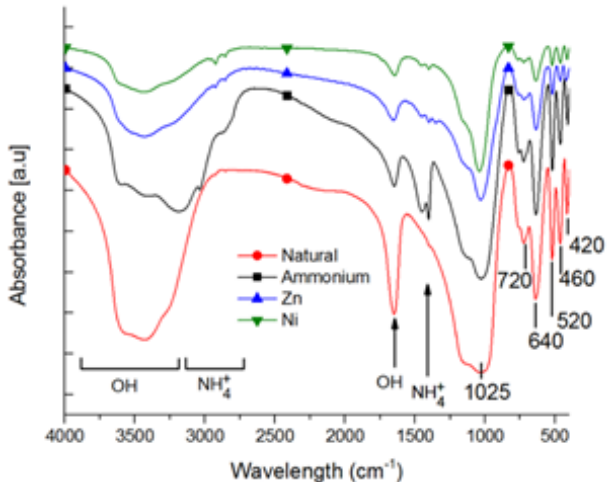

Fig. 5. FTIR spectra of natural CHA, NH4-CHA, Zn-CHA and Ni-CHA.

in the exchanged chabazite. These bands are very well pronounced and intensive for NH4-CHA, not present for natural CHA while for Ni- and Zn-CHA the low intensity of these bands (~1455, ~1400, ~1340, ~2930 and ~2850) suggests only minimal remains of NH_4^+.

The IR absorption bands associated with the chabazite framework vibrations are visible in the 400–1200 cm^{-1} range. As one can see the relative intensity and position of the six bands (420, 460, 520, 640, 720 and 1025) is not affected by the performed cation exchange. According to [34] CHA type phases are characterized by the presence of a triplet of peaks near 420, 455 and 510 cm^{-1}. These bands are clearly visible in our spectra at 420, 460, 520 cm^{-1} and thus FTIR data also supports that the conducted ion exchange is not affecting the structure of CHA. The meticulous assignment of the absorption bands related to the chabazite framework vibrations is usually associated to two types of vibrations representative for CHA building units (TO_4 tetrahedra, T = Si or Al). Those related to internal O–T–O symmetric, asymmetric stretching and bending and those that are characteristic for T–O–T linkages (involving a bridging oxygen atom). Thus the bands at 460, 640, 720 and 1025 cm^{-1} are associated to the O–T–O vibrations. The O–T–O asymmetric stretching vibrations occur at 1025 cm^{-1} while the symmetric stretching vibrations located at 640 and 720 cm^{-1} can be subdivided to internal (640 cm^{-1}) and external (720 cm^{-1}). The 460 cm^{-1} band is characteristic for tetrahedra O–T–O bending. The bands around 420 and 520 cm^{-1} are due to external linkage vibrations between tetrahedrons (T–O–T). The shoulder at ~1140 cm^{-1} results specifically from Si–O–Si asymmetric stretching mode.

The band at 1650 cm^{-1} reflects the bending vibration of H_2O molecules present in the CHA channels [35]. In addition the symmetric and asymmetric H_2O vibrations produce a broad peak in the 3000–3600 cm^{-1} region (also disclosing hydrogen bonding interactions).

Single crystal analyses were conducted for NH4-, Zn- and Ni-CHA. The structure solution and refinement allowed the location of the cations, ammonium (nitrogen atoms) and some of the H_2O molecules present in the CHA framework. The positions of ex-

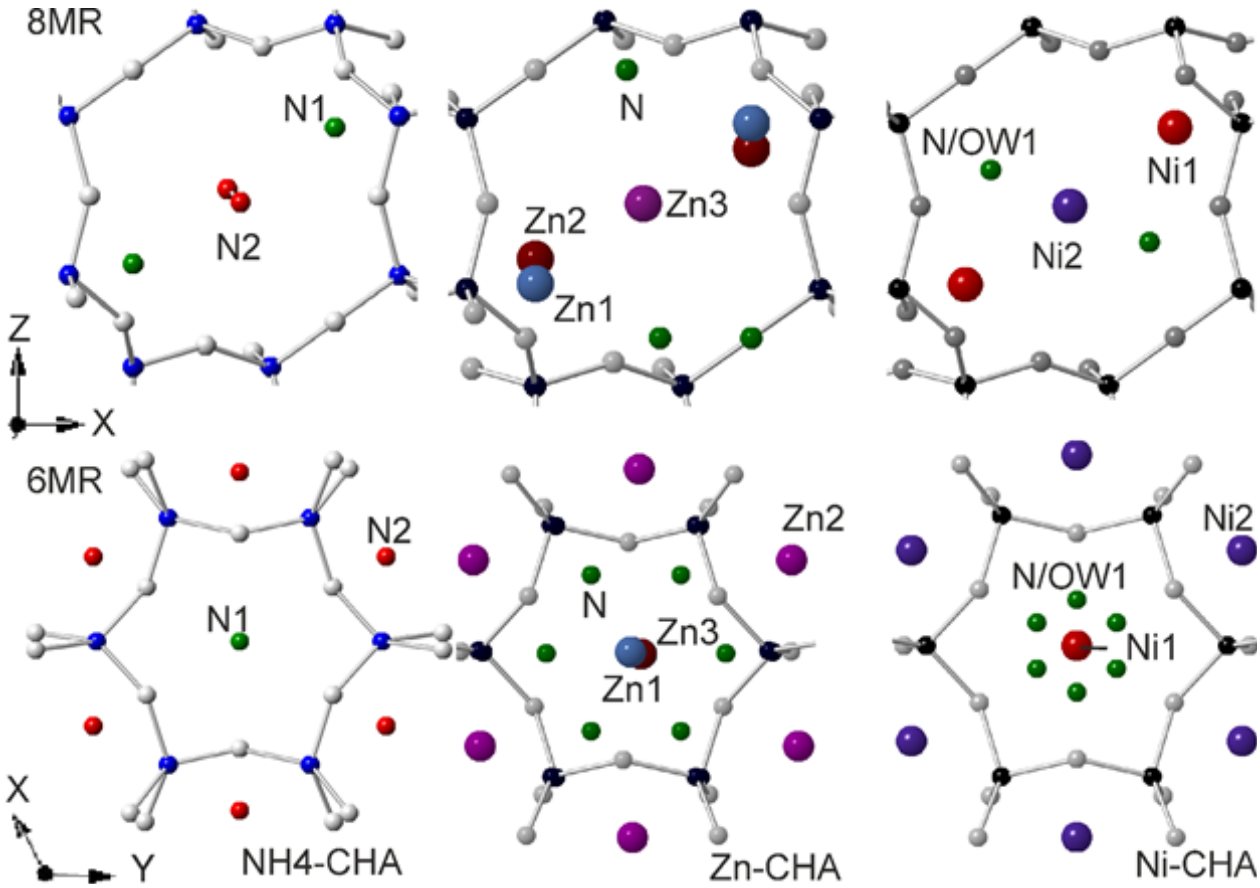

Fig. 6. Representation of NH_4^+, Zn and Ni cations location when viewed along 8MR and 6MR axes.

changeable cations, ammonium and H_2O molecules were obtained from difference Fourier. The location of hydrogen atoms from difference Fourier map was not always possible[1]. In the case of Zn-CHA and Ni-CHA the positions of hydrogen atoms associated with H_2O molecules were not determined. In the structure refinements, the occupancies of Si^{4+} and Al^{3+}, belonging to the aluminosilicate framework, were adjusted to the values obtained from the EDS chemical analysis while.

Previous structural studies of exchanged and dehydrated CHA have shown that there are several (three, four or five) "general" positions for the cations [36–39]. The present NH4-CHA refinement unveils the existence of two H_2O sites (OW1 and OW2) [38] and two ammonium (Nitrogen) sites (N1 and N2). Unfortunately NH_4^+ and H_2O are with similar MW, N and O scatter almost identically and there is no real possibility to differentiate between them from X-ray data – leaving the assignment to the observed electron density "open". Thus when viewed along the axis of the D6R prism (e.g. along *c*) N1 position seems to be in the center of the D6R (Fig. 6 second row) while in reality they are displaced out of the prism and are near the border of the $[4^{12}6^8 8^6]$ cavity (e.g. along *b*). The N2 nitrogen site is located at the center of the $[4^{12}6^8 8^6]$ cavity (Fig. 6 top row). Both nitrogen sites are close to a framework oxygen: N1 is near O2 (N1…O2 distance of 2.940 Å), N2 is near three oxygen atoms O1, O3 and O4 (N2…O1, N2…O3, N2…O4 distances are 3.20, 3.32 and 3.396 Å respectively). Interestingly N1, OW1 and OW2 participate also in a series of hydrogen bonding interactions producing a complex motif.

The refinement of "disordered" OW1 required some attention and ended with 34% occupancy, in accordance to its 12 fold symmetry operation replication near the borders of the D6R. The chemical compositions of NH4-CHA obtained from X-ray refinement and by EDS are quite similar, with values of 5.21 and 5.58 for N (based on 24 framework oxygen).

[1] The location of hydrogen atoms from X-ray is contestable as H features only one electron and the resulting scattering intensity is very weak and in addition is usually displaced toward the N or O atoms.

The results of the NH4-CHA refinement are comparable with those of Gualtieri and Passaglia [38].

According to the EDS data the subsequently conducted ion exchange (with 1M $ZnCl_2$ or $NiCl_2$ solutions) of the NH4-CHA form resulted in a partial displacement of ammonium molecules by Zn and Ni cations (as FTIR data suggest residual remains of ammonium). The refinement of the Zn- and Ni-CHA structures shows that the Zn^{2+} and Ni^{2+} cations occupy/displace the ammonium N1 and N2 sites. The ammonium, remaining Zn- and Ni-CHA structures, is displaced from the center of the rings, closer to the Si/Al framework (sharing its site with a H_2O molecule).

In Zn-CHA, the cations Zn^{2+} occupy three positions: Zn1 and Zn2 and Zn3. The resulting Zn1 site is in a threefold position when it is observed along *c*. Like N1 this position is situated out of the 6DR prism, and is near the border of the [$4^{12}6^8 8^6$] cavity. Position Zn2 corresponds to N2 (e.g. in the center of the [$4^{12}6^8 8^6$] cavity). Interestingly no suitable coordination H_2O molecules could be detected for Zn2. In Zn-CHA H_2O molecules are distributed into four positions OW1, OW2/N, OW3, and OW4 Position OW1 coordinates Z1 and Zn3 positions The H_2O molecules seem to be positioned concentrically/radially when viewed along the threefold axis of the D6R prism [40]. Position OW3 appears on the D6R axis (coordinates Z1 and Zn3 positions) while OW4 and OW2/N are displaced from the axis and closer to the border of the prism. These H_2O molecules, situated in the [$4^{12}6^8 8^6$] cavity are complementing the cation coordination. Position OW4 is the highly occupied in Zn-CHA (occupancy of 1), while OW1 OW2 and OW3 are less 0.32, 0.12 and 0.04 respectively. In Ni-CHA the cations (Ni^{2+}) occupy two positions Ni1 and Ni2. The sites correspond to N1 and N2 and thus to Zn1 and Zn2.

In Ni-CHA three water sites were located: OW1, OW2 and OW3 with occupancy of 0.21, 0.29, and 0.18 respectively. Positions OW1 and OW2 are analogous to those of the Zn-CHA. The distance OW1...Ni2 is 2.38 Å. Position OW3 is situated in the [$4^{12}6^8 8^6$] cavity with distance OW3...N1 2.68 Å.

CONCLUSIONS

Single crystals of natural chabazite were completely exchanged by NH4 cations. The subsequent ion exchange of the chabazite ammonium form (NH4-CHA) with 1M $ZnCl_2$ and $NiCl_2$ solution produced Zn-CHA and Ni-CHA forms. The exchange of NH_4^+ by Zn^{2+} and Ni^{2+} was not complete according to FTIR and EDS microanalyses. The Ni and Zn cations substitute easily two of the two ammonia positions observed in NH4-CHA: the position "N1" near the border of the [$4^{12}6^8 8^6$] cavity the other position "N2" at the center of the [$4^{12}6^8 8^6$] cavity. The remaining NH_4^+ in Zn-CHA and Ni-CHA shares a water position.

SUPPLEMENTARY MATERIALS

ICSD No 426116, 426117 and 426118 contains the supplementary crystallographic data for NH4-, Zn- and Ni-CHA respectively. Further details of the crystal structure investigation(s) may be obtained from Fachinformationszentrum Karlsruhe, 76344 Eggenstein-Leopoldshafen, Germany (fax: (+49)7247-808-666; e-mail: crysdata(at)fiz-karlsruhe.de, http://www.fiz-karlsruhe.de/request_for_deposited_data.html) on quoting the appropriate CSD number.

Acknowledgments: *This work was supported by ESF Grant BG05M2OP001-1.001-0008 and the Bulgarian National Science Fund through contract DRNF 02/1.*

REFERENCES

1. J. Shang, G. Li, R. Singh, P. Xiao, J. Z. Liu,P. A. Webley, *J. Phys. Chem. C*, **114**, 22025 (2010).
2. I. Georgieva, L. Benco, D. Tunega, N. Trendafilova, J. Hafner, H. Lischka, *J. Chem. Phys.*, **131** (2009).
3. R. K. Singh, P. Webley, *Adsorption-Journal of the International Adsorption Society*, **11**, 173 (2005).
4. V. Van Speybroeck, K. Hemelsoet, K. De Wispelaere, Q. Y. Qian, J. Van der Mynsbrugge, B. De Sterck, B. M. Weckhuysen, M. Waroquier, *Chemcatchem*, **5**, 173 (2013).
5. F. Goltl J. Hafner, *Microporous and Mesoporous Materials*, **166**, 176 (2013).
6. J. Shang, G. Li, R. Singh, Q. F. Gu, K. M. Nairn, T. J. Bastow, N. Medhekar, C. M. Doherty, A. J. Hill, J. Z. Liu,P. A. Webley, *J. Am. Chem. Soc.*, **134**, 19246 (2012).
7. D. P. Smith, *Water Environ. Res*., **83**, 373 (2011).
8. J. Weitkamp, *Solid State Ionics*, **131**, 175 (2000).
9. A. A. Zagorodni, Ion exchange materials: properties and applications, Elsevier, Amsterdam; Boston, 2007, 1st edn.
10. V. A. Nikashina, A. N. Streletsky, I. V. Kolbanev, I. N. Meshkova, V. G. Grinev, I. B. Serova, T. S. Yusupov, L. G. Shumskaya, *Clay Miner*., **46**, 329 (2011).
11. E. A. Eilertsen, S. Bordiga, C. Lamberti, A. Damin, F. Bonino, B. Arstad, S. Svelle, U. Olsbye, K. P. Lillerud, *Chemcatchem*, **3**, 1869 (2011).
12. M. Majdan, S. Pikus, Z. Rzaczynska, M. Iwan, O. Maryuk, R. Kwiatkowski, H. Skrzypek, *J. Mol. Struct*., **791**, 53 (2006).
13. G. J. D. Soler-illia, C. Sanchez, B. Lebeau, J. Patarin, *Chem. Rev.*, **102**, 4093 (2002).

14. M. V. Vener, X. Rozanska, J. Sauer, *Phys. Chem. Chem. Phys*., **11**, 1702 (2009).
15. K. Suzuki, G. Sastre, N. Katada,M. Niwa, *Phys. Chem. Chem. Phys*., **9**, 5980 (2007).
16. H. S. Shin, I. J. Jang, N. R. Shin, S. H. Kim, S. J. Cho, *Res. Chem. Intermediat*., **37**, 1239 (2011).
17. M. Hammes, M. Valtchev, M. B. Roth, K. Stowe,W. F. Maier, *Appl. Catal. B-Environ.*, **132**, 389 (2013).
18. V. Valtchev, G. Majano, S. Mintova, J. Perez-Ramirez, *Chem. Soc. Rev.*, **42**, 263 (2013).
19. F. Chen, Y. Liu, R. E. Wasylishen, Z. H. Xu, S. M. Kuznicki, *J. Nanosci. Nanotechno.*, **12**, 1988 (2012).
20. F. N. Ridha, Y. X. Yang, P. A. Webley, *Microporous and Mesoporous Materials*, **117**, 497 (2009).
21. E. P. Ng, D. Chateigner, T. Bein, V. Valtchev, S. Mintova, *Science*, **335**, 70 (2012).
22. T. Babeva, R. Todorov, B. Gospodinov, N. Malinowski, J. El Fallah, S. Mintova, *J. Mater. Chem.*, **22**, 18136 (2012).
23. C. Baerlocher, L. B. McCusker, D. H. Olson, Atlas of zeolite framework types, Elsevier B.V., 2007, 7-th edn.
24. B. de Gennaro, A. Colella, P. Aprea,C. Colella, *Microporous and Mesoporous Materials*, **61**, 159 (2003).
25. H. Lee, P. K. Dutta, *Microporous and Mesoporous Materials*, **38**, 151 (2000).
26. J. Cejka, H. V. Bekkum, A. Corma, F. Schuth, Introduction to Zeolite Science and Practice (vol. 168), Elsevier Science Bv, Amsterdam, 2007.
27. S. M. Kuznicki, C. C. H. Lin, J. Bian, A. Anson, *Clays Clay Miner.*, **55**, 235 (2007).
28. M. Bourgogne, J. L. Guth, R. Wey, *US Patent* 4 503 024 (1985).
29. M. Wojdyr, *J. Appl. Crystallogr.*, **43**, 1126 (2010).
30. Agilent, CrysAlis PRO, Agilent Technologies, UK Ltd, Yarnton, England, 2011.
31. G. M. Sheldrick, *Acta Crystallogr*., *A* **64**, 112 (2008).
32. J. Zhang, R. Singh,P. A. Webley, *Microporous and Mesoporous Materials*, **111**, 478 (2008).
33. M. Trzpit, S. Rigolet, J. L. Paillaud, C. Marichal, M. Soulard,J. Patarin, *J. Phys. Chem. B*, **112**, 7257 (2008).
34. E. M. Flanigen, L. B. Sand, Molecular Sieve Zeolites (Advances in Chemistry Series, vol. 101–102), American Chemical Society, Washington, D.C., 1971.
35. M. Falk, *Spectrochim. Acta A*, **40**, 43 (1984).
36. A. Alberti, E. Galli, G. Vezzalini, E. Passaglia, P. F. Zanazzi, *Zeolites*, **2**, 303 (1982).
37. L. J. Smith, H. Eckert,A. K. Cheetham, *J. Am. Chem. Soc.*, **122**, 1700 (2000).
38. A. F. Gualtieri, E. Passaglia, *Eur. J. Mineral.*, **18**, 351 (2006).
39. F. N. Ridha P. A. Webley, *Sep. Purif. Technol.*, **67**, 336 (2009).
40. A. Nakatsuka, H. Okada, K. Fujiwara, N. Nakayama, T. Mizota, *Microporous and Mesoporous Materials*, **102**, 188 (2007).

СТРУКТУРНИ ОСОБЕНОСТИ НА ПРИРОДЕН ХАБАЗИТ, МОДИФИЦИРАН ЧРЕЗ $ZnCl_2$ И $NiCl_2$

Л. Т. Димова[1], И. Пироева[2], С. Атанасова-Владимирова[2], Р. Русев[1], Б. Л. Шивачев[1]*

[1] Институт по минералогия и кристалография „Акад. Иван Костов“, Българска академия на науките, ул. „Акад. Георги Бончев“, бл. 107, 1113 София, България
[2] Институт по физикохимия, Българска академия на науките, ул. „Акад. Георги Бончев“, бл. 11, 1113 София, България

Постъпила март, 2018 г.; приета април, 2018 г.

(Резюме)

Монокристали от природен хабазит са модифицирани до получаването на NH_4^+, Zn^{2+} и Ni^{2+} форми, които са характеризирани чрез ЕДС/СЕМ, ДТА/ТГ, ИЧ, както и монокристален рентгеноструктурен анализ. Процедурата на модифициране включва последователното преминаване на изходния природен хабазит $(Na_{0.37}Ca_{1.56})Al_{3.63}Si_{8.36}O_{24}xH_2O$) в неговата амониева форма (NH4-CHA). Тази NH4-CHA форма се използва като изходна при последвалия йонен обмен с цинкови и никелови катиони. Йонният обмен се осъществява в 1M $ZnCl_2$ и $NiCl_2$ водни разтвори при 100 °C. ЕДС и ИЧ анализи, както и рентгеноструктурните проучвания, разкриха остатъци от амониеви катиони в Zn и Ni обменени форми. Структурните уточнения разкриват, че водните молекули, налични в структурата на хабазита, са склонни да заемат места, които обикновено са свързани с близки места на катионите. Тъй като катионните количества, необходими за компенсиране заряда на скелета, са ограничени, то и молекулите на водата също се приспособяват към тази особеност. Разпределението на водните молекули в 8-членния пръстен е от радиален тип.